Submitted: 03 April, 2024 Accepted: 25 June, 2024 Published: 03 May, 2025 DOI:10.22514/jocpd.2025.054

Journal of Clinical Pediatric Dentistry

ORIGINAL RESEARCH

Finite element analysis of initial displacement and periodontal stress distribution for inverted impacted maxillary central incisor by multiple traction directions

Yafen Zhu[1], Xiangtao Liu[1], Jian Wang[1], Jie Han[1], Mujia Li[1], Junzhuo Gou[1], Zhifang Wu[1],*

[1]Department of Pediatric Dentistry, Stomatology Hospital, School of Stomatology, Zhejiang University School of Medicine, Zhejiang Provincial Clinical Research Center for Oral Diseases, Key Laboratory of Oral Biomedical Research of Zhejiang Province, Cancer Center of Zhejiang University, Engineering Research Center of Oral Biomaterials and Devices of Zhejiang Province, 310000 Hangzhou, Zhejiang, China

***Correspondence**
11418288@zju.edu.cn
(Zhifang Wu)

Abstract

Background: Maxillary incisors are frequently encountered impacted which affect oral function, facial esthetics, and psychological and physical health. Orthodontic traction is preferred for the cases of incomplete root development. This study was aimed to evaluate and compare the initial displacement and stress differences among traction directions during the traction of different root development stages of inverted impacted central incisor based on 3-dimensional finite element analysis (FEA). **Methods**: Accordingly, the finite element models including maxilla, dentition, labially inverted impacted central incisor, periodontal ligaments, and traction appliance were constructed. Three root development stages of impacted incisor (1/3, 1/2, 2/3) were simulated. Three traction directions for each root length were applied by adjusting traction hook lengths of modified Nance arch appliance. **Results**: The impacted central incisor exhibited similar initial displacement tendencies of crown lingually and root labially rotated in all nine models. The maximum initial displacement ranged from 0.00336 to 0.00644 mm, where all were located at the incisal edge. The stress concentrated around lingual button was 0.37972 to 0.51023 MPa. Furthermore, the periodontal ligament (PDL) stress value of impacted incisor ranged from 0.01538 to 0.02612 MPa. The initial displacement and PDL stress decrease with the increase in root length of impacted incisor. With the same root length, the initial displacement and PDL stress were increased as the traction hook extended more to labial. Moreover, the average maximum initial displacement and PDL stresses of anchorage molars were 0.00010–0.00011 mm and 0.00044–0.00052 MPa. **Conclusions**: The traction direction and root development stage influenced the biomechanical effect of impacted incisor during traction. Additionally, the biomechanical effect of anchorage teeth existed but was inconspicuous.

Keywords

Inverted impacted central incisor; Modified Nance arch; Root development; Traction direction; 3-dimensional finite element analysis

1. Introduction

Maxillary incisors are the most frequently encountered impacted teeth second to impacted third molars and canines, with the prevalence varies from 0.04% to 2.0% [1, 2]. The localization and orientation of impacted maxillary central incisors varies. The incidence of labially inverted (crown directing upward and its palatal aspect facing labially) impacted incisors is higher than those of labially positioned and palatally impacted incisors [3–5]. Supernumerary teeth, acute trauma to primary tooth, and severe periapical inflammation of deciduous tooth are the possible impaction causes [6, 7]. Complications such as root resorption, eruption obstacle of adjacent teeth and dentigerous cyst can occur without timely and effective treatment [8]. Missing maxillary incisors may cause localized disturbances in developing dentition such as adjacent teeth migration and reduction in arch length, which subsequently affect patients' oral function, facial esthetics, and psychological and physical health [9].

Common clinical treatments of impacted incisors include surgical exposure with orthodontic traction, autotransplantation, extraction and prosthetic replacement [10, 11]. Orthodontic traction is preferred for cases with incomplete root development [12]. Traction button is bonded to the lingual side of inverted and horizontal impacted incisor's surgical exposure point. A modified Nance arch (MNA) device is generally used in early phase of traction cases having incomplete eruption of adjacent anterior teeth to bond brackets, or those with sufficient space for traction. It saves traction time for high-position impacted teeth and protects newly erupted permanent adjacent teeth [13, 14]. The length and direction of traction hook on MNA can be adjusted to attain desired movement for better therapeutics and less side-effects. Biomechanical characteristics such as force magnitude, application point, and direction of traction force are vital to achieve desired orthodontic treatment outcomes [15]. The position and direction of impacted teeth, root development stage, and dilaceration degree are also important to determine success rates of prognosis and treatment [16].

Finite elements analysis (FEA) is 3-dimensional (3D) engineering method to compare biomechanical properties under standard conditions by eliminating the individual variations. FEA in impacted tooth traction is commonly employed [17, 18] because of the practical difficulties in assessing and comparing under standardized conditions like position, dimensions, root development stage, morphology of impacted tooth, cancellous bone thickness, and anchorage unit in the clinical trials. FEA helps in determining optimal loading magnitude and directions that cause certain displacement, yield the least stress on impacted incisor, and minimize side effects during treatment. Most reported studies have focused on biomechanical changes of impacted incisors, while limited studies have investigated whether the force direction and root development stage have effect on inverted impacted central incisors, anchorage teeth, and adjacent teeth during traction by MNA with FEA.

The purpose of this study was to evaluate and compare the biomechanical changes of impacted central incisor, anchorage molars, and adjacent teeth under traction by MNA. It was hypothesized that traction direction and root development stage had influence on the biomechanical effect of impacted incisor, while inconspicuous changes were noted in anchorage and adjacent teeth during traction. The specific aims of the study were: (1) to measure and compare the initial displacements and von Mises stresses of impacted central incisor with different root development stages via different traction directions; (2) to evaluate biomechanical changes of anchorage molars and adjacent teeth in corresponding conditions.

2. Material and methods

2.1 Participant enrollment and acquisition of CBCT image data

A cone beam computed tomography (CBCT) scan of randomly selected 7-year-old male patient having inverted impacted incisor seeking orthodontic treatment at our institution was used in the study. CBCT scan (NewTom, Quantitative Radiology, Verona, Italy) was conducted with following parameters: 3 mA, 110 kV, voxel size of 0.3 mm, and scanning area of 15 $\times$ 15 cm.

Inclusion criteria: (1) Presence of unilateral maxillary central incisor unerupted and labially inverted impacted; (2) The contralateral central incisor erupted to normal position. Exclusion criteria: (1) Presence of untreated endodontic or periodontal disease; (2) Temporomandibular joints disorder symptom; (3) History of maxillary surgery, trauma or tumor, and maxillary developmental deformities; (4) Other systemic diseases.

2.2 3D Finite element model construction and analysis

2.2.1 Model construction and assembly

A 3D geometric model of maxilla and maxillary dentition was created by Mimics 21.0 (Materialise Software, Materialise Corps, Leuven, Belgium) after importing the raw Digital Imaging and Communications in Medicine (DICOM) format data from CBCT scan. The model was then further surface finished, its features were optimized using Geomagic Studio 2021 (Geomagic, Morrisville, NC, USA), and saved in step format. The impacted tooth root formation was manually adjusted to stimulate root development stage (*i.e.*, 1/3, 1/2 and 2/3). The periodontal ligament (PDL) with 0.18 mm thickness was molded on the outer surface of the root.

A non-meshed model was imported to 3D modeling software, Solidworks Premium 2021 (Dassault Systemes, Solidworks Corps, Providence, RI, USA) to replicate traction appliances for testing, which consisted of (a) Bands (5-mm height and 0.2-mm thickness) placed on maxillary first molars of both sides; (b) A modified Nance arch containing 1.2-mm diameter stainless steel wire, acrylic resin connector, and stainless traction hook connected between the first molar bands. The stainless traction hook was designed of three varied lengths for simulating traction directions; (c) A 2-mm diameter and 1-mm height button was designed to bond on 1-mm to incisal edge of impacted tooth lingual surface.

The components (maxilla, maxillary dentition, impacted central incisors, periodontium, lingual button and intraoral traction appliance) of each model were assembled in Solidworks and saved as x-t format file.

2.2.2 Material properties and meshing

The assembled file was imported to ANSYS Workbench 2021 R1 (ANSYS, Canonsburg, PA, USA) to create 3D finite element model. Each model was meshed to tetrahedral elements with ten nodes. The maximum number of nodes were employed to create a mesh structure of the finest quality to approach clinically valid findings. Nine models were constructed based on above stimulations, and included in this study. Table 1 encompassed material properties wherein anatomic components and appliances were assumed as the isotropic and homogeneous materials [17, 19, 20]. The nine models were listed in Table 2. Table 3 depicted elements and nodes numbers for each model. Fig. 1 showed the traction appliance with varied traction hook lengths and root development stages from occlusal and sagittal view.

2.2.3 Boundary constraints and finite element analysis

A full constraint was employed on superior and posterior regions of maxilla to stimulate its boundary condition for attaching to surrounding zygomatic, palatal, and sphenoid bones. Resultantly, they had no rotation or translation movement. A traction force of 0.6 N was applied between the lingual button and traction hook via virtual spring unit simulation in ANSYS for all investigated schemes [17, 20].

Nine loading setups were analyzed respectively in nine models aforementioned. The maximum initial displacement and

TABLE 1. Material properties used in the simulations of the geometric models.

Structures	Young's modulus (MPa)	Poisson coefficient
Tooth	20,000	0.30
PDL	0.68	0.45
Alveolar bone	13,700	0.30
Lingual button	114,000	0.34
Stainless steel	200,000	0.30
Acrylic resin	2700	0.30

PDL: periodontal ligament.

TABLE 2. Nine models with different root development stages of impacted inverted incisor and traction hook lengths of traction appliance.

Models	Root development stage	Traction appliance
Model 1	1/3	Type I
Model 2	1/3	Type II
Model 3	1/3	Type III
Model 4	1/2	Type I
Model 5	1/2	Type II
Model 6	1/2	Type III
Model 7	2/3	Type I
Model 8	2/3	Type II
Model 9	2/3	Type III

equivalent stress (von Mises) resulting from the force applied by traction appliance of the impacted central incisor, anchorage molars and adjacent teeth, as well as those in the labial and lingual PDL, were calculated and analyzed.

3. Results

3.1 Study flow diagram

Flow diagram in Fig. 2 illustrated the current 3D FEA. Maximum initial displacements and von Mises stresses were analyzed for the impacted central incisor, anchorage molars, adjacent incisors, and those in PDL.

3.2 Maximum initial displacements and von Mises stresses of impacted central incisor

The initial displacement trend of crown and root of the impacted central incisor was opposite in all models, *i.e.*, crown to lingual and root to labial (Fig. 3). The maximum and minimum displacements were observed respectively in the incisal edge and labial side of tooth cervix.

The initial displacement and stress were decreased with the increase in root length of impacted central incisor. With the same root length, the initial displacement was increased and stress was decreased as the traction hook extended more to labial. The initial displacements of Model 1–9 were 0.00534, 0.00577, 0.00644, 0.00451, 0.00461, 0.00544, 0.00336, 0.00363 and 0.00404 mm, respectively. Impacted central incisor in Model 3 revealed the highest initial displacement, while that of in Model 7 was the minimum. Model 1–3, Model 4–6, Model 7–9 were progressively increased. However, the initial displacement was sequentially decreased with the increase in tooth root length, *i.e.*, the initial displacement of impacted central incisor with 1/3 root formation was greater than that with 1/2, and impacted incisor with 2/3 root formation showed the least initial displacement.

The von Mises stress for impacted central incisor in all Models (Fig. 3) was concentrated in the lingual side of crown, around lingual button and was decreasing towards root apex. The von Mises stress decreased gradually with the increase in root length and traction hook from Model 1 to 9, *i.e.*, 0.51023, 0.49826, 0.47169, 0.46648, 0.4635, 0.42822, 0.41665, 0.40502 and 0.37972 MPa, respectively (Fig. 3).

3.3 Displacements and von Mises stresses in the PDL of impacted central incisor

Displacements in the PDL of impacted central incisor from Model 1 to 9 were 0.00404, 0.004170, 0.00434, 0.00316, 0.00316, 0.00319, 0.00242, 0.00244 and 0.00246 mm, respectively. For von Mises stress in the PDL of impacted central incisor in all Models, the cervical area of root labial surfaces was concentrated with the maximum value, while the value was minimum around the middle of root labial surfaces Fig. 4). The von Mises stresses in periodontal lingual and labial sides in Model 1–9 were 0.02154, 0.02333, 0.02612, 0.02119, 0.02172, 0.02597, 0.01538, 0.01684 and 0.01918 MPa, respectively. The maximum stress was decreased and range of minimum stress was increased with the increase in root length. Moreover, the maximum stress was increased along with the traction hook extended more to labial for the same root length.

3.4 Maximum initial displacements and von Mises stresses of anchorage molars and those in the PDL

As displayed in Fig. 5, the displacement and von Mises stress of anchorage molars on both sides showed similar tendency. An opposite initial displacement trend was depicted in the crown and root of anchorage molars in all models, *i.e.*, crown to lingual and root to labial. The maximum initial displacement was on the lingual side of crown. Furthermore, the von Mises stress distribution pattern exhibited the same initial displacement. The initial displacement and stress were decreased with the increase in length of impacted central incisor root on both sides of anchorage teeth. With the same impacted central incisor root length, the initial displacement was increased and stress decreased as the traction hook extended more to labials. Anchorage right and left molar initial displacements were 0.00007 to 0.00008 mm, and 0.00012 to 0.00013 mm, respectively. Moreover, von Mises stresses in anchorage right and left molar were 0.02885 to 0.03522 MPa, and 0.07055 to 0.08015 MPa, respectively. The periodontal maximum von Mises stress was concentrated in the cervical area of palatal root of anchorage molars, which dwindled toward the palatal root apex and buccal root (Fig. 6). Both right and left molars

TABLE 3. The number of finite element analysis elements and nodes per model.

	Models								
	1	2	3	4	5	6	7	8	9
Number of nodes									
Tooth	65,666	65,666	65,666	65,277	65,277	65,277	65,438	65,438	65,438
PDL	168,948	168,948	168,948	170,235	170,235	170,235	171,804	171,804	171,804
Alveolar bone	45,377	45,377	45,377	45,390	45,390	45,390	45,718	45,718	45,718
Traction device	33,963	34,064	34,194	33,924	34,016	34,155	33,907	33,999	34,138
Number of elements									
Tooth	36,281	36,281	36,281	36,065	36,065	36,065	36,128	36,128	36,128
PDL	83,291	83,291	83,291	83,924	83,924	83,924	84,707	84,707	84,707
Alveolar bone	26,147	26,147	26,147	26,138	26,138	26,138	26,328	26,328	26,328
Traction device	17,721	17,767	17,836	17,695	17,735	17,810	17,684	17,724	17,799

PDL: periodontal ligament.

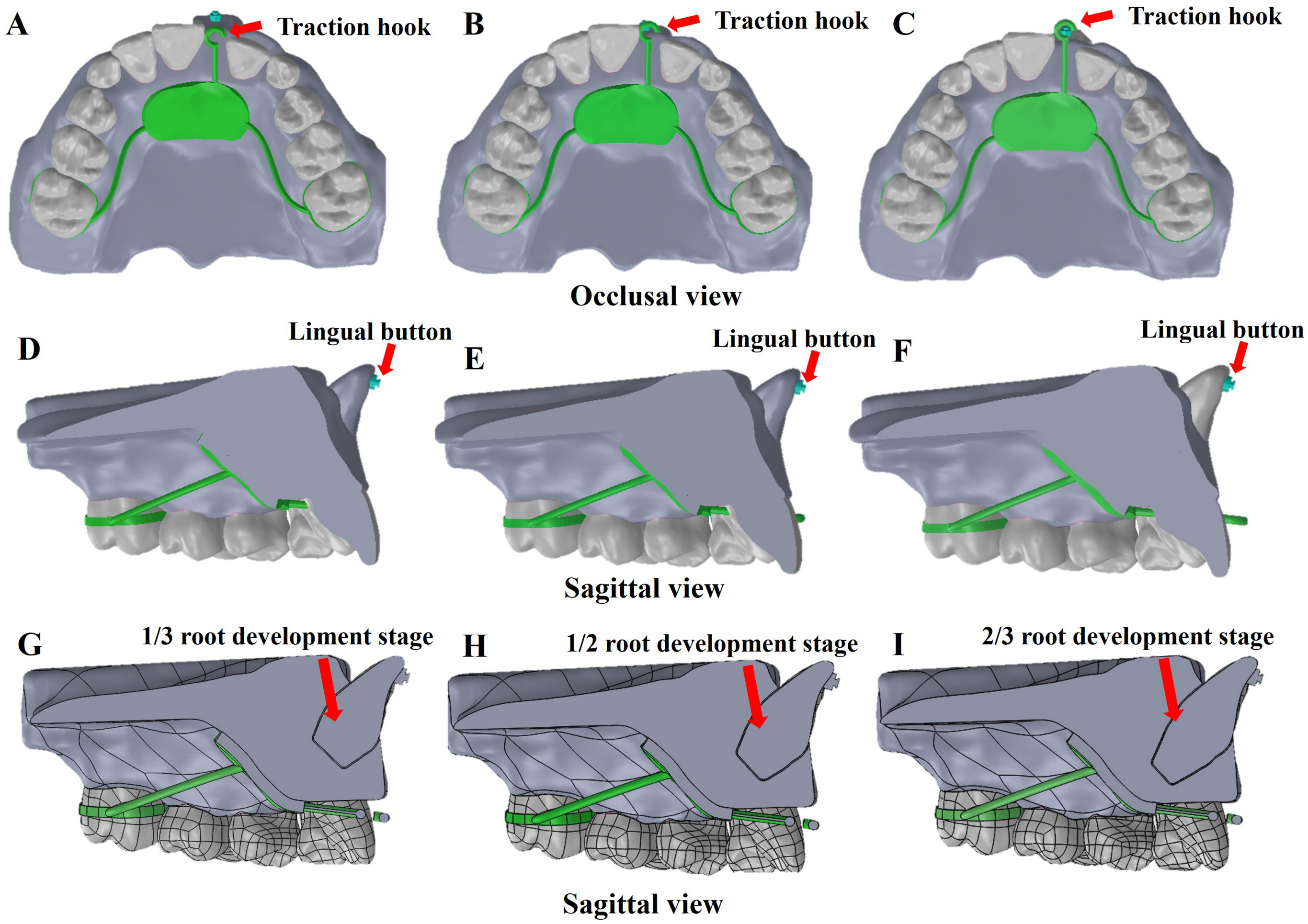

FIGURE 1. Modified Nance arch traction appliance and root development stage of impacted incisor from occlusal and sagittal view. (A) Type I traction appliance. (B) Type II traction appliance. (C) Type III traction appliance. The difference between the three traction appliance types was the different length of traction hook (2 mm hook length difference between each type). (D–F) The lingual button was bonded to the lingual surface of impacted incisor. (G) 1/3 root development stage. (H) 1/2 root development stage. (I) 2/3 root development stage.

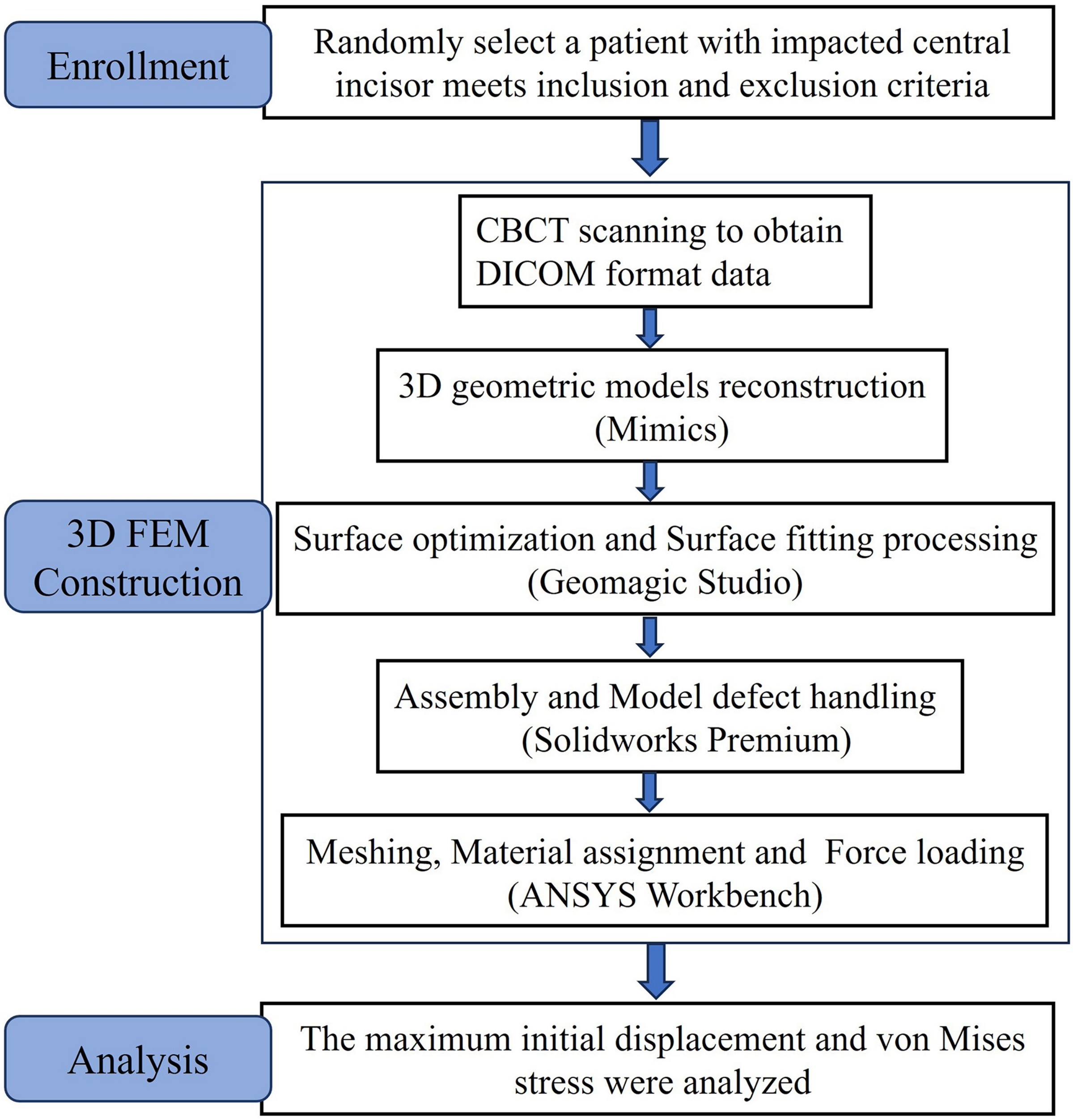

FIGURE 2. Study flow diagram. CBCT: cone beam computed tomography; 3D: 3-dimensional; FEM: finite element model; DICOM: digital imaging and communications in medicine.

exhibited similar distribution pattern. The average lingual and labial PDL von Mises stresses of anchorage right and left molars from Model 1 to 9 were 0.00044, 0.00047, 0.00051, 0.00044, 0.00045, 0.00051, 0.00044, 0.00047 and 0.00052 MPa, respectively.

3.5 Maximum initial displacements of adjacent anterior teeth

The maximum initial displacements of adjacent anterior teeth were negligible (Table 4). The values of adjacent contralateral incisor and ipsilateral lateral incisor were 9.1695×10^{-6} to 1.3378×10^{-5} mm, and 1.8392×10^{-5} to 2.2678×10^{-5} mm, respectively.

4. Discussion

The appropriate magnitude and traction force direction, as well as the displacement tendency and amount of stress in response are the vital aspects of impacted teeth traction. The biomechanical differences were evaluated by simulating the labially inverted impacted central incisor traction using MNA appliance. This study was aimed to evaluate the initial displacements and stress amount of impacted central incisor, adjacent teeth, and anchorage molars during the traction by employing FEA. Moreover, it aimed to provide references for clinicians regarding the clinical treatment protocols. FEA results delivered quantified information related to force direction through appliance design and root development stages. It was demonstrated that initial displacement and PDL stress distribution of impacted incisors under MNA traction were

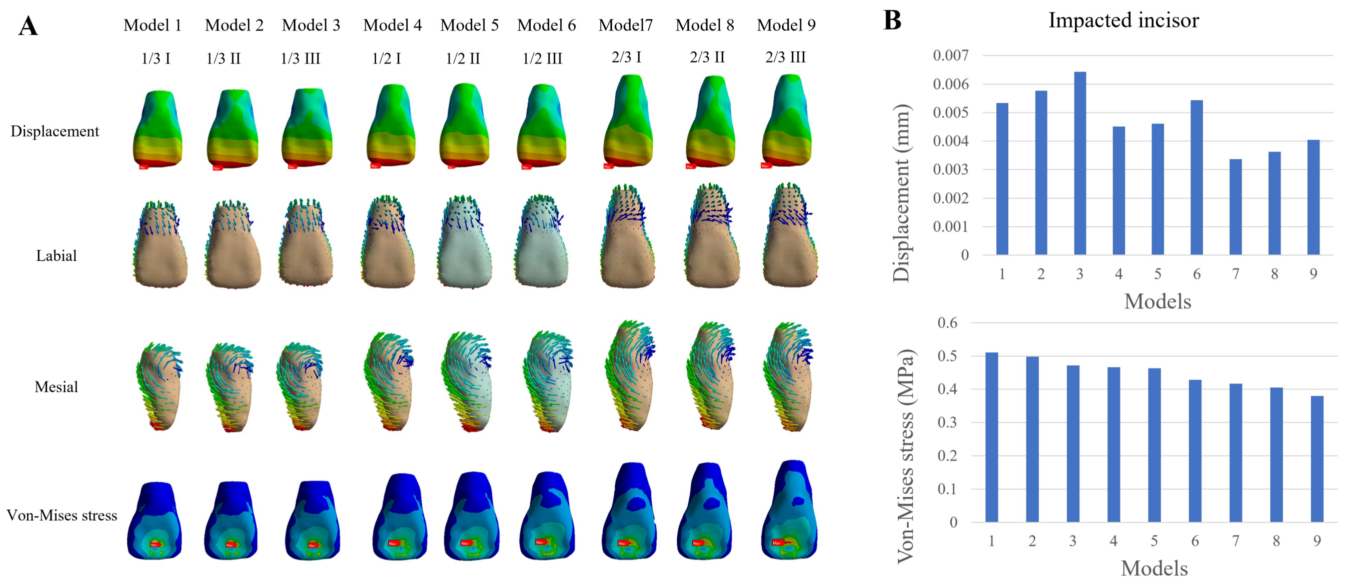

FIGURE 3. Initial displacement and von Mises stress cloud maps (A) and values (B) of inverted impacted central incisor of 9 three-dimensional finite element models. Blue to red reflects lower to higher displacement and stress.

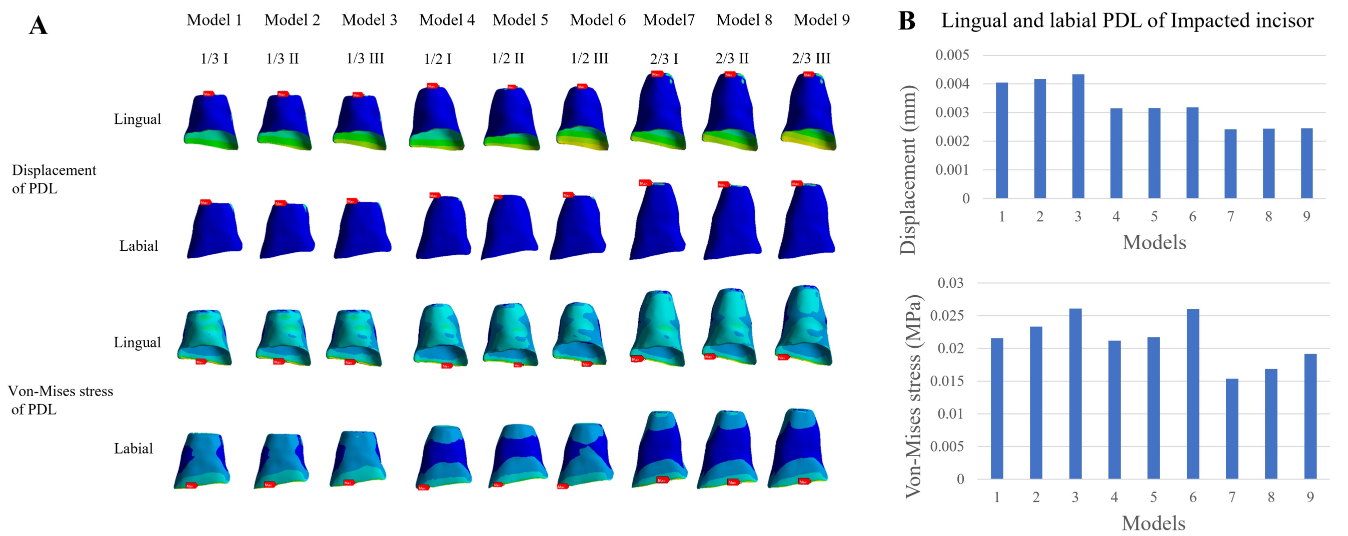

FIGURE 4. Initial displacement and von Mises stress cloud maps (A) and values (B) in the lingual and labial PDL of inverted impacted central incisor of 9 three-dimensional finite element models. PDL: periodontal ligament.

changed with the root development stage and length of traction hooks. The initial displacement, stress of impacted incisor and those in PDL were decreased with increase in root length. With the same root length, initial displacement was increased and stress decreased as the traction hook extended more to labial. Additionally, under the same root length, PDL stress were greater with longer traction hook length. More labial force maybe suitable at the initial stages of inverted impacted incisor traction. Different simulations caused little varied displacement and stress for anchorage teeth. The biomechanical effects on adjacent teeth were not obvious.

The opposite displacement trends of crown and root were seen for impacted incisor. The incisal regions yielded higher stress than cervical and apex regions in all models to reflect the initial tipping movement. The cervical area of root labial surfaces was the concentrated one with maximum PDL stress, while it was minimum around the middle. The maximum PDL stress was decreased and minimum stress range was increased with the increase in root length.

The success rate of prognosis and treatment of impacted teeth was dependent on both impacted teeth and traction modes. It included the impacted teeth position, root development stage, root morphology, available space in dental arch, Hertwig's epithelium activity, force magnitude, traction force direction, *etc.* [15, 21]. Maxillary central incisors with eruption disturbances exhibited less root length and tooth volume compared to those erupted normally in same individual [22]. The impacted inverted maxillary incisors often developed into root dilaceration because of the limitations of palatal bone plate, especially in later-age dental

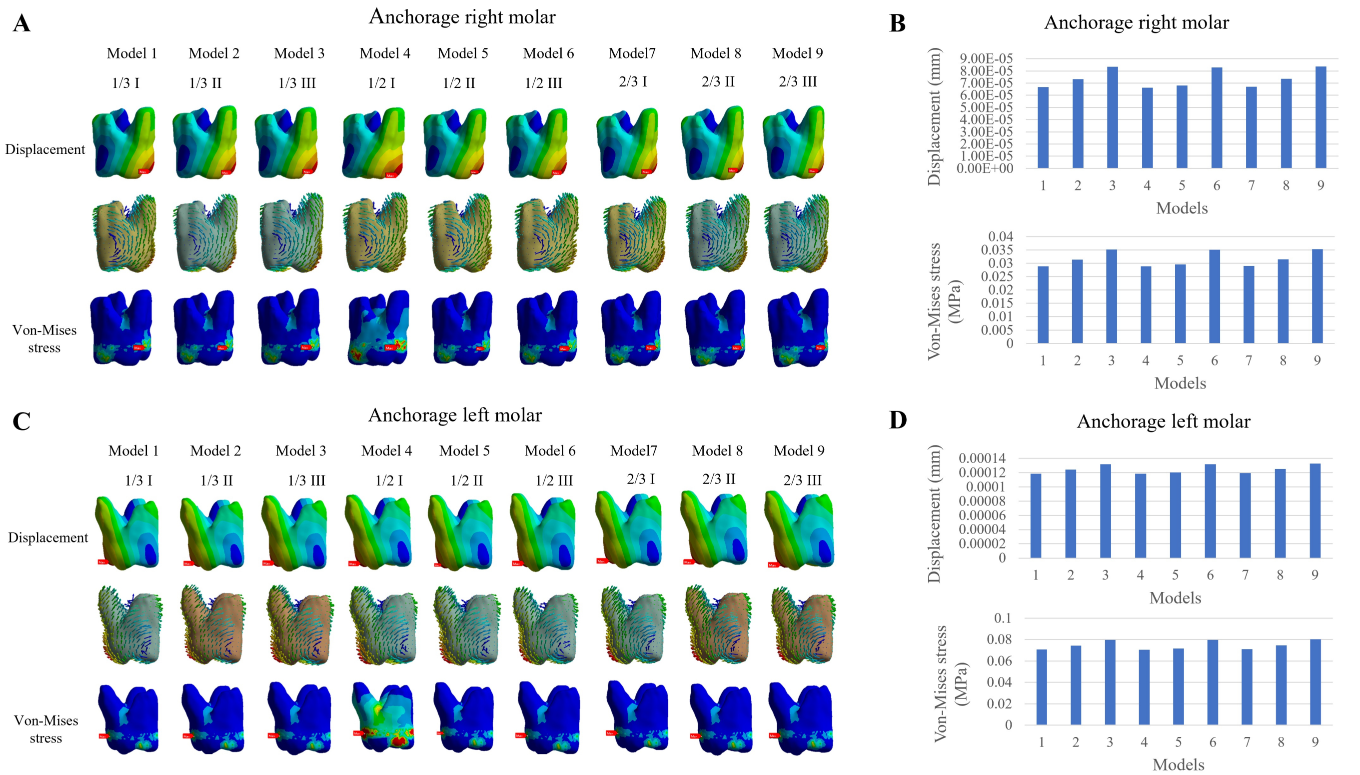

FIGURE 5. Initial displacement and von Mises stress cloud maps (A,C) and values (B,D) of right and left anchorage molars of 9 three-dimensional finite element models.

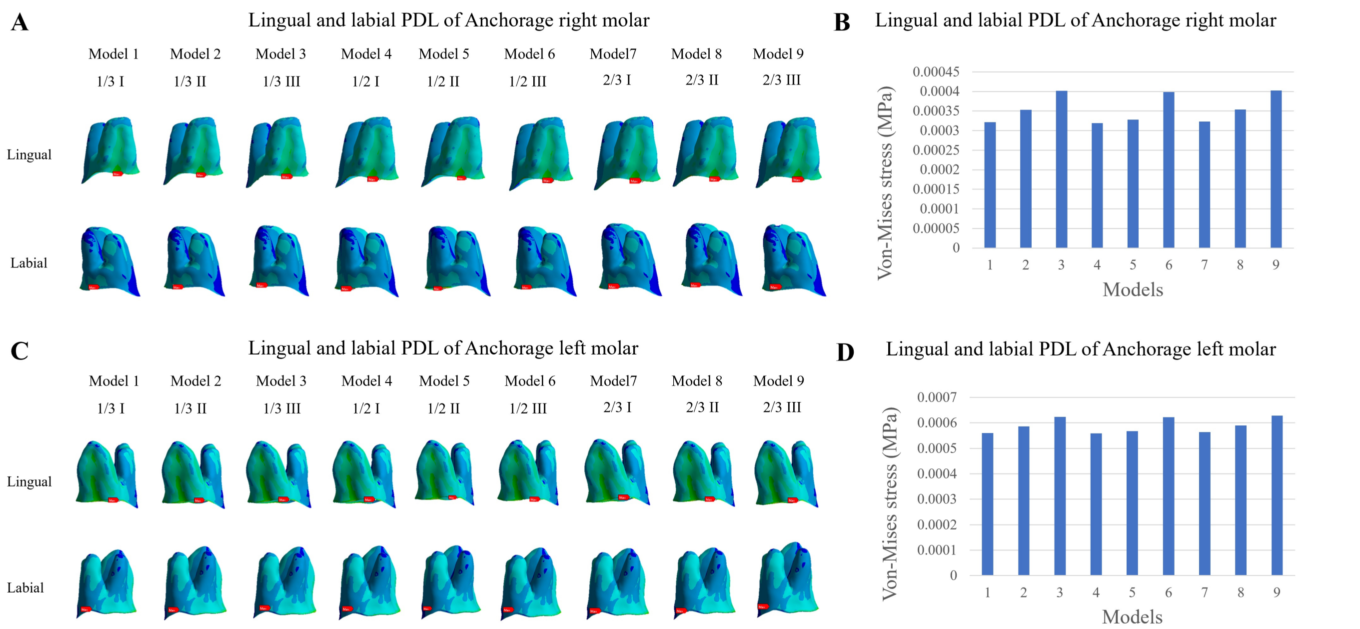

FIGURE 6. von Mises stress cloud maps (A,C) and values (B,D) in the lingual and labial PDL of right and left anchorage molars of 9 three-dimensional finite element models. PDL: periodontal ligament.

group [23, 24]. Orthodontic traction for impacted incisor in mixed dentition promoted root development and alveolar bone remodeling with good periodontal and endodontic conditions [25]. However, deformed root morphology increased the risk of root resorption and labial alveolar bone loss during traction, which influenced the functional and aesthetic outcomes [26]. The traction incisors had higher potential of root development with greater changes in apical foramen width and root length compared to the control. However, the root length of traction incisors was shorter than that of control [27]. Therefore, the labially inverted impacted central incisors are recommended to be treated early due to sufficient apical blood supply and

TABLE 4. Displacement (mm) of adjacent contralateral incisor and ipsilateral lateral incisor.

	Adjacent contralateral incisor	Adjacent ipsilateral lateral incisor
Model	Displacement (mm)	Displacement (mm)
1	9.1695×10^{-6}	1.8392×10^{-5}
2	9.8741×10^{-6}	1.9253×10^{-5}
3	1.0957×10^{-5}	2.0473×10^{-5}
4	9.8109×10^{-6}	1.8747×10^{-5}
5	1.0031×10^{-5}	1.9016×10^{-5}
6	1.1738×10^{-5}	2.0913×10^{-5}
7	1.1145×10^{-5}	2.0262×10^{-5}
8	1.2022×10^{-5}	2.1254×10^{-5}
9	1.3378×10^{-5}	2.2678×10^{-5}

strong tissue regeneration ability to promote root development and achieve better root apex morphology [12, 28]. The biomechanical changes of anchorage and adjacent teeth also need pay more attention to in impacted teeth traction treatment because of adverse effects such as unfavorable tooth movement or undesirable external root resorption may occur when using improper traction methods. The requirements of anchorage were high for labially inverted impacted incisor due to long traction eruption path and high resistance, because orthodontic treatment was completed by flipping the root above 90° inside the alveolar bone. However, patients in early stage of mixed dentition period had few available anchorage teeth. Early traction by MNA was preferred [29], however, majority of cases required additional techniques such as 2×4 mechanics to align the dentition and create space for impacted teeth [30]. Our result showed that initial tipping movement of impacted incisor occurred, and longer the root length under same traction force, smaller displacement was performed on crown with smaller PDL stress, which may due to farther was center of rotation (CR) from incisal tip. Loading position and traction force direction influence the displacement and maximum stress because they affected tooth movement pattern by influencing Moment/Force (M/F) in orthodontic movement. The CR position determined the amount and direction of tooth movement [31]. Thus, for inverted impacted central incisors, the button bonding position should be close to the incisal edge for facilitating tooth tipping movement with light force. CR also depended on root length in addition to loading position and traction force direction [32]. However, it is worth noting that CR usage to describe tooth displacement was sensitive with large standard deviations and might lead to inadequate interpretations. Displacement vectors were more feasible in describing initial and longitudinal tooth displacements [33]. A force of 0.6 N was selected in this study because light traction force (0.35 to 0.6 N) was suitable in reducing stress at impacted incisor apex and cortical alveolar bone. It thus reduced the root resorption or lessened the impact of normal root development [14].

However, some limitations required to be addressed. Firstly, it was limited for evaluating the initial response towards single-valued force, and von Mises stress was used to evaluate the loading and stress analyses in the current FEA. The maximum (tensile stress) and minimum principal stress (compressive stress) of alveolar cortical bone around central incisor were also important variables for conductive outcomes. Moreover, the inverted impacted teeth at high location used closed eruption technique for less periodontal recession in clinical scenario [34]. Its traction direction adjustment was hard due to gingival mucosal resistance. Furthermore, the straight single-rooted impacted incisor with fixed location was only considered, whereas the incisor with dilacerated or multi-rooted root were also possible scenarios. Lastly, this work was a 3-dimensional FEA conducted by simulating conditions using software, which lacked continuity and comparison with the finished clinical cases.

The current study would provide references and help clinicians to determine relative optimal loading directions causing certain displacement and yielding less stress for different root formation stages of impacted incisor. Future research would require dynamic time-dependent motion analysis and include more relevant influencing factors (*e.g.*, force magnitude, root morphology, impaction angulation, and vertical impaction height) through FEA, and combine FEA with clinical longitudinal and quantitative studies to draw more generalizable outcomes.

5. Conclusions

Despite the limitations of this study, both traction direction and root development stage have influence on biomechanical effect of impacted central incisor during traction by modified Nance arch. However, the biomechanical changes of anchorage and adjacent teeth was inconspicuous. MNA traction appliance is useful for orthodontic traction cases in the early dentition phase, and the more labial force maybe suitable at initial stages of inverted impacted incisor traction. In summary, clinicians should consider personalized rather than universal treatment protocols for inverted impacted central incisors traction.

AVAILABILITY OF DATA AND MATERIALS

The data that support the findings of the current study are available from the corresponding author and the first author upon reasonable request.

AUTHOR CONTRIBUTIONS

YFZ and ZFW—contributed to conception and design. XTL, JW, JH, MJL and JZG—contributed to acquisition, analysis, and interpretation. YFZ—contributed to draft manuscript. ZFW, YFZ and MJL—critically revised manuscript. All authors read and approved the final manuscript.

ETHICS APPROVAL AND CONSENT TO PARTICIPATE

The protocol for this study was approved by the institutional ethics review board of the Affiliated Stomatology Hospital, Zhejiang University School of Medicine (No. 2023-101). Informed consent was obtained from legal guardians.

ACKNOWLEDGMENT

Not applicable.

FUNDING

This work was supported by the National Natural Science Foundation of China (NSFC, Grant/Award No. 82101046).

CONFLICT OF INTEREST

The authors declare no conflict of interest.

REFERENCES

[1] Tan C, Ekambaram M, Yiu CKY. Prevalence, characteristic features, and complications associated with the occurrence of unerupted permanent incisors. PLOS ONE. 2018; 13: e0199501.

[2] Thirasupa N. Orthodontic management of a horizontally impacted maxillary incisor in an adolescent patient. American Journal of Orthodontics and Dentofacial Orthopedics. 2023; 163: 126–136.

[3] Du W, Chi J, He S, Wu G, Pan W, Wang Y, *et al*. The position and morphology characteristics of multiple impacted anterior teeth in the unilateral maxillary area: a retrospective study based on cone-beam computed tomography. American Journal of Orthodontics and Dentofacial Orthopedics. 2022; 162: 907–916.

[4] Wu G, He S, Chi J, Sun H, Ye H, Bhikoo C, *et al*. The differences of root morphology and root length between different types of impacted maxillary central incisors: a retrospective cone-beam computed tomography study. American Journal of Orthodontics and Dentofacial Orthopedics. 2022; 161: 548–556.

[5] Hui J, Niu Y, Jin R, Yang X, Wang J, Pan H, *et al*. An analysis of clinical and imaging features of unilateral impacted maxillary central incisors: a cross-sectional study. American Journal of Orthodontics and Dentofacial Orthopedics. 2022; 161: e96–e104.

[6] Flores MT, Onetto JE. How does orofacial trauma in children affect the developing dentition? Long-term treatment and associated complications. Dental Traumatology. 2019; 35: 312–323.

[7] Seehra J, Mortaja K, Wazwaz F, Papageorgiou SN, Newton JT, Cobourne MT. Interventions to facilitate the successful eruption of impacted maxillary incisor teeth due to the presence of a supernumerary: a systematic review and meta-analysis. American Journal of Orthodontics and Dentofacial Orthopedics. 2023; 163: 594–608.

[8] Hu H, Hu R, Wu G, Sun C. The evaluation of lateral incisor adjacent to treated labial inversely impacted maxillary central incisor: a retrospective follow-up study. American Journal of Orthodontics and Dentofacial Orthopedics. 2023; 164: 57–66.

[9] Seehra J, Alshammari A, Wazwaz F, Papageorgiou SN, Newton JT, Cobourne MT. Periodontal outcomes associated with impacted maxillary central incisor and canine teeth following surgical exposure and orthodontic alignment: a systematic review and meta-analysis. European Journal of Orthodontics. 2023; 45: 584–598.

[10] Ayers E, Kennedy D, Wiebe C. Clinical recommendations for management of mesiodens and unerupted permanent maxillary central incisors. European Archives of Paediatric Dentistry. 2014; 15: 421–428.

[11] Shi R, Zhou Z, Li P, Shi L, Sun H, Bai Y. *In situ* rotation surgery for correction of growing, inversely impacted maxillary central incisors. American Journal of Orthodontics and Dentofacial Orthopedics. 2021; 159: 536–544.

[12] Sun H, Hu R, Ren M, Lin Y, Wang X, Sun C, *et al*. The treatment timing of labial inversely impacted maxillary central incisors: a prospective study. The Angle Orthodontist. 2016; 86: 768–774.

[13] Hu H, Hu R, Jiang H, Cao Z, Sun H, Jin C, *et al*. Survival of labial inversely impacted maxillary central incisors: a retrospective cone-beam computed tomography 2-year follow-up. American Journal of Orthodontics and Dentofacial Orthopedics. 2017; 151: 860–868.

[14] Mannathoko-Molefshe B, Hu R. Management of impacted maxillary central incisor: modified Nance arch application. The Journal of Contemporary Dental Practice. 2015; 16: 415–421.

[15] Zeno KG, Mustapha S, Ayoub G, Ghafari JG. Effect of force direction and tooth angulation during traction of palatally impacted canines: a finite element analysis. American Journal of Orthodontics and Dentofacial Orthopedics. 2020; 157: 377–384.

[16] Bhikoo C, Xu J, Sun H, Jin C, Jiang H, Hu R. Factors affecting treatment duration of labial inversely impacted maxillary central incisors. American Journal of Orthodontics and Dentofacial Orthopedics. 2018; 153: 708–715.

[17] Lena Sezici Y, Gediz M, Akış AA, Sarı G, Duran GS, Dindaroğlu F. Displacement and stress distribution of Kilroy spring and nickel-titanium closed-coil spring during traction of palatally impacted canine: a 3-dimensional finite element analysis. Orthodontics & Craniofacial Research. 2020; 23: 471–478.

[18] Zeno KG, El-Mohtar SJ, Mustapha S, Ghafari JG. Finite element analysis of stresses on adjacent teeth during the traction of palatally impacted canines. The Angle Orthodontist. 2019; 89: 418–425.

[19] Elsayyad AA, Abbas NA, AbdelNabi NM, Osman RB. Biomechanics of 3-implant-supported and 4-implant-supported mandibular screw-retained prostheses: a 3D finite element analysis study. Journal of Prosthetic Dentistry. 2020; 124: 68 e1–68 e10.

[20] Xia Q, He Y, Jia L, Wang C, Wang W, Wang C, *et al*. Assessment of labially impacted canines traction mode with clear aligners *vs.* fixed appliance: a comparative study based on 3D finite element analysis. Frontiers in Bioengineering and Biotechnology. 2022; 10: 1004223.

[21] Shi X, Sun X, Wang X, Zhang C, Liu Y, Quan J, *et al*. The effect of the root dilaceration on the treatment duration and prognosis of unilateral impacted immature maxillary central incisors. American Journal of Orthodontics and Dentofacial Orthopedics. 2023; 163: 79–86.

[22] Jeong Y, Shin J, Park S, Jeong T, Lee E. Morphometric comparison and prognostic analysis of permanent maxillary central incisors with eruption disturbances—a cross-sectional study. Children. 2024; 11: 307.

[23] Sun H, Wang Y, Sun C, Ye Q, Dai W, Wang X, *et al*. Root morphology and development of labial inversely impacted maxillary central incisors in the mixed dentition: a retrospective cone-beam computed tomography study. American Journal of Orthodontics and Dentofacial Orthopedics. 2014; 146: 709–716.

[24] Lana Mattiello FD, Deon Rizzatto SM, Macedo de Menezes L, Araújo EA, Kim KB, Martinelli de Lima E. Dimensional and morphologic characteristics of unilateral impacted maxillary central incisors. American Journal of Orthodontics and Dentofacial Orthopedics. 2022; 162: 340–347.

[25] Cheng C, Li X, Liu H. Evaluation of the orthodontic treatment outcome in patients with impacted maxillary central incisor in the mixed dentition. Chinese Journal of Stomatology. 2016; 51: 263–268. (In Chinese)

[26] Sameshima GT, Sinclair PM. Predicting and preventing root resorption: part I. Diagnostic factors. American Journal of Orthodontics and Dentofacial Orthopedics. 2001; 119: 505–510.

[27] Zhang W, Chen W, Chen ZF. Clinical study of a adjustable movable re-

tractor for maxillary labially inverted impacted central incisor. Shanghai Journal of Stomatology. 2023; 32: 193–197. (In Chinese)

[28] Lyu J, Lin Y, Lin H, Zhu P, Xu Y. New clues for early management of maxillary impacted central incisors based on 3-dimensional reconstructed models. American Journal of Orthodontics and Dentofacial Orthopedics. 2018; 154: 390–396.

[29] Yordanova G, Gurgurova G. Impacted upper central incisors—frequency and factors complicating the treatment protocol. Folia Medica. 2021; 63: 405–412.

[30] Hirschhaut M, Weinstein C, Alarcon C, Flores-Mir C. Clinical guidelines for the surgical/orthodontic management of impacted maxillary central incisors based on a decision tree. Compendium of Continuing Education in Dentistry. 2023; 44: 510–515; quiz 516.

[31] Smith RJ, Burstone CJ. Mechanics of tooth movement. American Journal of Orthodontics. 1984; 85: 294–307.

[32] Tanne K, Nagataki T, Inoue Y, Sakuda M, Burstone CJ. Patterns of initial tooth displacements associated with various root lengths and alveolar bone heights. American Journal of Orthodontics and Dentofacial Orthopedics. 1991; 100: 66–71.

[33] De Pauw G, Dermaut L, De Bruyn H. The value of the centre of rotation in initial and longitudinal tooth and bone displacement. European Journal of Orthodontics. 2003; 25: 285–291.

[34] Marek I, Jankova A, Starosta M, Novosad M, Kucera J. Comparison of spontaneous eruption and modified closed eruption technique with palatal traction in alignment of impacted maxillary central incisor teeth. Progress in Orthodontics. 2023; 24: 17.

How to cite this article: Yafen Zhu, Xiangtao Liu, Jian Wang, Jie Han, Mujia Li, Junzhuo Gou, *et al*. Finite element analysis of initial displacement and periodontal stress distribution for inverted impacted maxillary central incisor by multiple traction directions. Journal of Clinical Pediatric Dentistry. 2025; 49(3): 89-98. doi: 10.22514/jocpd.2025.054.